6998 *Biochemistry* **2009,** *48,* 6998–7008
DOI: 10.1021/bi900396h

BIOCHEMISTRY
including biophysical chemistry & molecular biology
Article

Direct Kinetic Evidence That Lysine 215 Is Involved in the Phospho-Transfer Step of Human 3-Phosphoglycerate Kinase†

Andrea Varga,‡ Corinne Lionne,*,§ Perrine Lallemand,§ Judit Szabó,‡ Nancy Adamek,∥ Christian Valentin,§ Mária Vas,‡ Tom Barman,§ and Laurent Chaloin§

‡*Institute of Enzymology, Biological Research Center, Hungarian Academy of Sciences, Karolina Út 29, H-1113 Budapest, Hungary,* §*Centre d'études d'agents Pathogènes et Biotechnologies pour la Santé (CPBS), UMR 5236, CNRS, Université Montpellier 1, Université Montpellier 2, Institut de Biologie, 4 bd Henri IV, CS69033, 34965 Montpellier Cedex 2, France, and* ∥*Department of Biosciences, University of Kent, Canterbury, Kent CT2 7NJ, United Kingdom*

Received March 9, 2009; Revised Manuscript Received June 16, 2009

ABSTRACT: 3-Phosphoglycerate kinase (PGK) is a promising candidate for the activation of nucleotide analogues used in antiviral and anticancer therapies. PGK is a key enzyme in glycolysis; it catalyzes the reversible reaction 1,3-bisphosphoglycerate + ADP ↔ 3-phosphoglycerate + ATP. Here we explored the catalytic role in human PGK of the highly conserved Lys 215 that has been proposed to be essential for PGK function by a transient and equilibrium kinetic study with the active site mutant K215A. By the stopped-flow method we show that the kinetics of substrate binding and the associated protein isomerization steps are fast and identical for the wild-type PGK and mutant K215A. By the use of a chemical sampling method (rapid quench flow) under multiple and single turnover conditions and in both directions of the reaction, we show that the rate-limiting step with wild-type PGK follows product formation (presumably product release), whereas with the mutant it is the phospho-transfer step itself that is rate-limiting. Mutant K215A has a low inherent phosphotransferase activity, and to explain this, we carried out a molecular modeling study. This suggests that with the mutant the conserved Arg 65 replaces the missing Lys 215 by helping to position the transferable phospho group during the reaction. Molecular dynamics simulations suggest that in the mutant the closed conformation of the enzyme is stabilized by a salt bridge between Asp 218 and Arg 170 rather than Arg 65 in the wild-type PGK.

3-Phosphoglycerate kinase (PGK; EC 2.7.2.3)[1] catalyzes the reversible transfer of the phospho group between 1,3-bisphosphoglycerate (bPG) and ADP:

$$\text{bPG} + \text{ADP} \leftrightarrow \text{PG} + \text{ATP}$$

PGK is a key enzyme in glycolysis (in the forward reaction) and carbon fixation in plants (in the backward reaction) and is present in all living organisms studied so far (*1*). Furthermore, PGK appears to be involved in other biological processes. For instance, since it is relatively nonspecific for its nucleotide substrates, it is thought to be a component of the cascade of cellular kinases that activate nucleoside prodrugs to the pharmacologically active nucleoside triphosphates (refs *2* and *3* and references cited therein). PGK has also been reported to act in tumor angiogenesis as a disulfide reductase (*4*). Because of its multiple roles, it seemed important to establish a detailed knowledge of the reaction pathway of this enzyme.

PGK is a globular protein with two distinct domains: the N-domain that contains the bPG or PG binding site (*5*) and the C-domain that binds ADP (*6*) or ATP (*7*). It is thought that on the binding of both substrates the two domains approximate, a process ("hinge bending") that leads to a closed conformation of the enzyme and which is necessary for phospho-transfer to occur (*8*). However, to date, all available crystal structures of mammalian PGKs (*5*, *7*, *9*−*12*) are in an open conformation, even in the presence of the substrates. Nevertheless, there are two PGK crystal structures [from *Trypanosoma brucei* (*13*) and *Thermotoga maritima* (*14*)] in which the protein is in a closed conformation. In the open structures, the highly conserved Lys 215, located in the C-domain, is about 10 Å from the PG binding site (PDB structures 1HDI and 1VJC), which is too far to allow phospho-transfer. In the presence of PG and ADP, to form the

†This publication was prepared within the framework of the Hungarian−French Intergovernmental Scientific and Technological Cupertino Program and was supported by a grant from Egide (Balaton Program No. 14100ZF) and by the Hungarian Foundation of Research and Innovative Technology (OMFB-00493/2007, Project No. F-43/2006). The financial support provided by grants from the Agence Nationale de Recherches sur le Sida and OTKA NK 77978 from the Hungarian National Research Foundation are also gratefully acknowledged. A.V. was supported by a short-term FEBS fellowship.

*To whom correspondence should be addressed. Telephone: +33-467-600-595. Fax: +33-467-604-420. E-mail: corinne.lionne@univ-montp1.fr.

[1]Abbreviations: ANS, 1-anilinonaphthalene-8-sulfonic acid; bPG, 1,3-bisphosphoglycerate; GA, genetic algorithm; hPGK, human PGK; HPLC, high-performance liquid chromatography; MD, molecular dynamics; PG, 3-phosphoglycerate; PGK, 3-phospho-D-glycerate kinase or ATP:3-phospho-D-glycerate 1-phosphotransferase (EC 2.7.2.3); SAXS, small-angle X-ray scattering; TBAB, tetrabutylammonium bromide; wt, wild-type; yPGK, yeast PGK.

 Published on Web 06/16/2009

abortive E·PG·ADP, a complex that is thought to mimic the catalytic E·bPG·ADP, there appears to be a substantial structural change that may mimic the "hinge bending" process by which Lys 215 moves to within H-bonding distance of one of the phosphate oxygens of PG [*T. brucei* PGK (*13*)]. This interaction, which helps to connect the C-domain (nucleotide site) to the N-domain (PG site), could play a role in stabilizing the closed form of PGK. We note that in a recent infrared study on yeast PGK (yPGK), White et al. (*15*) came to the conclusion that the structure of the catalytic complex is "closer" than that of the abortive complex.

As pointed out by Auerbach et al. (*14*), with the enzyme from *T. maritima*, Lys 215 is well positioned in that with Arg 38 it escorts the 1-phospho group of bPG to ADP by stabilizing the putative pentacoordinate state of the phospho group. The proposal that Lys 215 is catalytically important is consistent with the large reduction of the steady-state rate of human PGK (hPGK) when it is replaced by alanine to give mutant K215A (*16*). Flachner et al. (*16*) estimated that at 20 °C k_{cat} in the forward reaction (k_{cat}^{F}, ATP formation) was 0.03% that of the wild-type PGK (wt PGK) and in the backward reaction (k_{cat}^{B}, bPG formation) 0.06%. They also showed that whereas the affinity of mutant K215A for ADP was similar to that of wt PGK, the affinity for ATP, which carries the transferable phospho group, was decreased 5-fold.

From these several works, it has been proposed that Lys 215 plays a key role in the phospho-transfer process catalyzed by PGK. However, it has not yet been shown whether the lysine is involved in the phospho-transfer step itself or with the steps associated with substrate binding. We note that from SAXS experiments (*17*) the involvement of Lys 215 in domain closure appears to be excluded.

A way to obtain information on an enzyme reaction pathway is to perturb the system under study. One can perturb by changing the experimental conditions. Cryoenzymology is an example of this technique which involves two perturbants: temperature and antifreeze (*18*). We have exploited cryoenzymology with yPGK by including methanol in the reaction medium and working at 4 °C, and by this means, we were able to build a seven-step reaction pathway and to obtain estimates for its rate constants (*19*, *20*). One can also perturb by the use of substrate analogues. We applied this approach to hPGK by comparing the kinetics of the interaction with D-ADP with that of its mirror image L-ADP (*3*). Finally, one can perturb by enzyme active site mutagenesis.

Here we put to the test the proposed catalytic importance of Lys 215 by a comparison of the chemical reaction pathways of wild-type hPGK and its mutant K215A by quench-flow and stopped-flow methods. We have already put forward a reaction pathway for yeast PGK (*20*), and we analyze our kinetic data by the same pathway (Scheme 1).

In our experiments, the starting enzyme material was E*·bPG in the forward and E*·PG in the backward reaction. In Scheme 1, there are three types of steps: formation of collision complexes (steps 1 and 5), protein isomerizations (steps 2 and 4), and the step of interest here, the phospho-transfer step (step 3).

We show that with mutant K215A, whether in the forward or backward reaction, the phospho-transfer step itself is very slow and clearly rate-limiting.

EXPERIMENTAL PROCEDURES

Proteins and Reagents. wt hPGK, its mutant K215A, and bPG were prepared as described in ref *16*. ADP and ATP were purchased from Sigma-Aldrich, and PG was from Roche Diagnostics.

Experimental Conditions. The experiments were carried out in a buffer that contained 20 mM triethanolamine, pH 7.5, 0.1 M potassium acetate, and 1 mM free Mg^{2+} as magnesium acetate (*21*). Because of its high turnover rate, it is difficult to study the transient kinetics of PGK, even at 4 °C, but by including 30% methanol in the buffer the kinetics were slowed down to measurable rates (*20*). Stock solutions of nucleotides contained an equivalent amount of Mg^{2+}. "ADP" and "ATP" refers to MgADP and MgATP, respectively.

Steady-State Kinetics and Product Measurements. The overall steady-state parameters of wt PGK and its mutant K215A with respect to the nucleotide substrates were obtained at 4 °C and in buffer that contained 30% methanol. The kinetics of the formation of product were obtained by the assay of ATP (in the forward reaction) and ADP (in the backward reaction) by HPLC.

In the forward reaction, phospho-transfer was initiated by the addition of the enzyme (final concentration 0.1 μM for wt PGK, 10 μM for mutant K215A) to buffer that contained bPG (50 μM) and variable concentrations of ADP. The reaction mixtures were aged while samples were removed at different times, quenched in 6.25% trichloroacetic acid, and clarified by centrifugation, and the supernatant was adjusted to pH 5.5 with NaOH. The quenched samples were diluted 10-fold with the HPLC mobile phase (see below) and 0.1 mL portions subjected to reverse-phase chromatography. The amounts of nucleoside di- and triphosphate were obtained from isocratic HPLC on a reverse-phase C18, ODS Hypersil 150 × 4.6 mm, 3 μm column (Thermo Electron) at a flow rate of 1 mL/min. The mobile phase was 125 mM potassium phosphate buffer, pH 5.5, 10 mM tetrabutylammonium bromide (TBAB), and 10% acetonitrile (adapted from ref *22*). The column was connected to a Waters chromatography system that includes a 1525 binary pump, a 717 plus autosampler, and an absorbance detector (2487 dual wavelengths) for the detection of adenosine di- and triphosphate (at 259 nm). The HPLC peaks were analyzed with the Waters Breeze software package that allows calculating the nucleotide concentrations. The steady-state constants were estimated from the ATP formed vs time plots (results not illustrated). Under our experimental conditions, less than 5% of the bPG hydrolyzed spontaneously during the incubation of the reaction mixtures (not more than 10 min).

Scheme 1: Reaction Pathway for PGK[a]

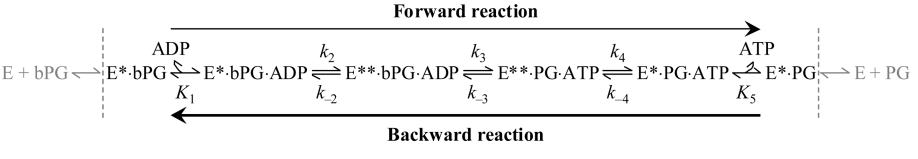

[a] E represents PGK, the asterisks denote different protein conformations, and K_i are dissociation constants.

In the backward reaction, phospho-transfer was initiated by the addition of enzyme to buffer that contained PG (5 mM) and variable concentrations of ATP, and after quenching in acid, the ADP produced was measured by HPLC as described above.

Fluorescence Stopped-Flow Transient Kinetics. The experiments were carried out in a thermostatically controlled SF-DX2 stopped-flow apparatus (Tgk Scientific, U.K.). The wavelengths used were 295 nm for excitation and >320 nm for emission. Full experimental details and the precautions taken are in Gondeau et al. (*3*).

Quench-Flow Transient Kinetics. The experiments were carried out in home-built thermostatically controlled quench-flow apparatuses. In the forward reaction, PGK and bPG were in the "enzyme" syringe and ADP was in the "substrate" syringe of the quench-flow apparatus. Equal volumes of each (typically 70−150 μL) were mixed in the apparatus, the reaction mixtures were aged in the time range milliseconds to several seconds and quenched in 6.25% trichloracetic acid, and the ATP and ADP were measured by HPLC as described above. Zero time points were obtained by mixing 0.1 mL of PGK·bPG solution with 0.2 mL of acid and then 0.1 mL of ADP solution. End time points were obtained by mixing 0.1 mL of PGK·bPG solution with 0.1 mL of ADP solution, incubating for 30 min at room temperature, and quenching with 0.2 mL of acid before HPLC analysis. In the backward reaction, PGK and PG were in the "enzyme" syringe and ATP and PG in the "substrate" syringe with the same procedure used as for the forward reaction. The concentrations of PG used (typically 100 μM to 5 mM) were well above its K_d: 0.7 ± 0.2 μM for wt PGK (*3*) and 0.5 ± 0.2 μM for mutant K215A (data not shown).

Molecular Modeling, Docking of ADP and ATP, and Dynamics Simulation. The model structures of wt hPGK and mutant K215A in a closed conformation were built from the *T. brucei* PGK (13PK) crystal structure using the Modeller release program 8v2 (*24*). In order to improve the quality of the models and to determine side chain orientations, their stereochemistry was optimized with Modeller by using an energy minimization/dynamics procedure of the objective function (geometric restraints and nonbonded contacts). All of the hydrogen atoms were included in the models, including those that define the correct ionization state of histidine, using the hbuild command of the Charmm program (Harvard University). For all of the docking, the water molecules in the crystal structures were retained. The VMD program (*25*) was used to analyze the interactions and to measure the distances between the atoms in the models and bound ADP or ATP.

The docking of ADP or ATP into the PGK models was carried out by the use of GOLD (Genetic Optimization for Ligand Docking, CCDC software limited) v4 that uses a genetic algorithm (GA). This method permits a certain amount of flexibility: partial with the protein and complete with the ligand. For each of 50 independent GA runs, a default maximum number of 100000 genetic operations was carried out with the use of default operator weights and a population size of 100 chromosomes. The atom chosen as target to define the nucleotide binding site was the nitrogen atom of Pro 338 with an active site radius of 15 Å in combination with scrutiny for a cavity. The second substrate, PG, was docked prior to ADP or ATP as described above except that the target atom was the α-carbon of Gly 392. The magnesium ion was coordinated with a tetrahedral geometry with the two oxygen atoms of Asp 374 and two water molecules. Mg ion should be coordinated with six ligands, as can be clearly seen in the 1.6 Å resolution crystal structure of the MgADP binary complex of *Bacillus stearothermophilus* PGK [1PHP (*6*)]. When the resolution of the X-ray structure is not high enough, not all of the ligands of the Mg ion can be seen, and in the present modeled structure two water molecules could be missing.

Chemscore was used as a scoring function, and the different docking poses were analyzed by the clustering method (complete linkage) from the rmsd matrix of ranking solutions. This allows defining the conformation that ranked the best prior energy minimization. Briefly, the potential energy was minimized in three steps using the Charmm program (500 steps of steepest descent followed by 5000 steps of a conjugate gradient [tolerance 0.01 kcal/(mol·Å)] without applying any constraint).

Molecular dynamics (MD) simulation was carried out using NAMD (*26*) and the CHARMM all-atom parameter set 22 (*27*). Protein−ligand complexes (wt and mutant K215A) surrounded by crystal water molecules were immersed in a water box of thickness of 10 Å in *x*, *y*, *z* directions from the protein surface, and they were replicated by periodic boundary conditions. The solvated systems were energy minimized using 500 steps of conjugate gradient as described above. Electrostatic and van der Waals interactions were treated with an r-dependent dielectric constant and a switch function applied between 10 and 12 Å. The particle mesh Ewald method was used to calculate electrostatic interaction with a grid spacing of 1 Å. MD simulations were carried out at 300 K for 1 ns with an integration time step of 1 fs at constant temperature and pressure using a Nosé-Hoover piston. A time scale of 1 ns was selected as it is thought to be sufficient to observe side chain motions.

RESULTS AND DISCUSSION

Here, our aim was to provide firm kinetic evidence for the proposed key importance of Lys 215 in the phospho-transfer reaction of PGK by, in particular, determining the rate-limiting step on the reaction pathway of mutant K215A. The strategy was, first, to compare the kinetics of the initial steps in the forward reaction of mutant K215A with those of wt PGK by exploiting the intrinsic fluorescence of PGK that occurs on ADP binding. We also investigated the effect of PG on the ADP binding kinetics to form the corresponding E·PG·ADP, a complex that has been proposed to be a model for the catalytic E·bPG·ADP (*13*, *28*).

Second, it was to characterize chemically and kinetically the intermediates following substrate binding by exploiting the quench-flow method in which reaction mixtures are aged from a few milliseconds to several tens of seconds and quenched in acid, and then a product is measured by a specific analytical method. When the time course of product formation includes a transient "burst" phase of product, one can come to conclusions not only on the rate-limiting step on the overall reaction pathway of the enzyme but also on the identity and kinetic properties of enzyme product intermediates (*29*). Here, we investigated the transient kinetics of formation of ATP in the forward and of ADP in the backward reactions of wt hPGK and its mutant K215A.

But first, we checked on the overall structures of PGK and its mutant under our experimental conditions (30% methanol and 4 °C).

CD Studies. The far-UV spectra of wt PGK and mutant K215A in buffer with or without methanol are illustrated in Supporting Information. With the wt PGK, the spectrum that we obtained in the methanol-free buffer is in agreement with that obtained by Szabó et al. (*17*). It is noteworthy that the spectra of the mutant are very similar to those of wt PGK, whether or not

the solvent contained methanol. Thus, each spectrum is characteristic of an α helix-rich protein with two minima centered at 207 and 222 nm and a maximum at 193 nm. This similarity is evidence that the secondary structure of PGK is not greatly affected by the mutation, a lack of effect that is supported by the finding that the magnitude of the fluorescence signals observed on the addition of ADP to the mutant is similar to that with wt PGK (see below). Furthermore, the similarity of the CD spectra shows that 30% methanol does not perturb significantly the conformation of PGK, whether wild-type or mutant.

Equilibrium Studies. The effect of the concentration of ADP on the fluorescence signal of mutant K215A is illustrated in Supporting Information, and the dissociation constants, K_d, obtained are in Table 1. In the absence of PG, the affinity for ADP was hardly affected by the mutation. The affinities measured here, in a buffer that contained 30% methanol and at 4 °C, are in agreement with those obtained by Flachner et al. (*16*) in a methanol-free buffer and at 20 °C: for wt PGK $K_d = 28$ μM; for mutant K215A $K_d = 45$ μM.

It is noteworthy that PG decreased equally (about 7-fold) the affinities of wt PGK and its mutant for ADP (Table 1). This effect, termed "substrate antagonism", has been observed for pig muscle (*28*) and human (*3*) wt PGKs.

We also obtained estimates for the affinities of wt PGK and its mutant for PG. With the wild-type, although the amplitude of the fluorescence signal was low, we were able to obtain an estimate for K_d for PG of 0.7 μM (*3*). However, with the mutant, the amplitude was too low to be exploited, and instead, a fluorescence titration method with ANS (*23*, *30*) as the probe was used to obtain an estimate of the K_d for PG: 0.5 μM (data not shown).

Kinetic Studies on the Forward Reaction (ATP Formation). Thermodynamically, this is the favorable reaction, and free ATP production goes to near completion.

(A) Kinetics of the Initial Steps: Stopped-Flow Studies. As with wt PGK (*3*), the kinetics of the decrease in tryptophan fluorescence observed when ADP interacts with mutant K215A fitted well to a single exponential giving a rate constant k_{obs} (time courses not illustrated). The dependence of k_{obs} on the ADP concentration is in Figure 1. Also included in the figure is the dependence in the presence of PG. In each case the dependence was fitted to a straight line of slope k_+ and intercept on the k_{obs} axis k_-. As with wt PGK (*3*), we interpret these parameters by a two-step binding process for ADP (Scheme 2) (see Single Turnover Experiments for details).

With reference to Scheme 2, $k_{obs} = k_+[ADP] + k_-$, where $k_+ = k'_2/K'_1$ and $k_- = k'_{-2}$ (see Supporting Information for details). We summarize in Table 1 the estimates for k_+ and k_- with the PGK mutant together with those for the wild-type enzyme. From these experiments, we conclude that mutant K215A binds ADP with kinetics that are similar to those of wt PGK, both in the absence and in the presence of PG. We note that the presence of PG results in an increase of k_-. This is the kinetic basis of "substrate antagonism", as concluded earlier with wt PGK (*3*).

That the mutation of Lys 215 has little effect upon the ADP binding kinetics is reasonable; it implies that the binding of ADP to PGK does not involve this residue, which is reserved for the γ-phosphate of ATP. This is in agreement with Flachner et al. (*16*), who showed that whereas the mutation of Lys 215 weakens the binding of ATP, it hardly affects that of ADP. On the other hand, we show here that, as with wt PGK, PG decreased the affinity of K215A for ADP. Thus, it seems that the communication between the PG and ADP sites (*28*) is unaffected by the mutation of Lys 215. This result is consistent with the occurrence of domain closure in mutant K215A as derived from the SAXS measurements (*17*), since both substrate antagonism (*28*) and domain closure (*8*) are mediated through interdomain communication.

Table 1: ADP Binding Kinetics to wt PGK and Mutant K215A in the Presence or Absense of PG from Equilibrium (K_d) and Stopped-Flow Studies (k_+, k_-)[a]

$$E(\cdot PG) \underset{K'_1}{\overset{ADP}{\rightleftharpoons}} E(\cdot PG)\cdot ADP \underset{k'_{-2}}{\overset{k'_2}{\rightleftharpoons}} E^*(\cdot PG)\cdot ADP$$

kinetic parameters	wt PGK[b]	mutant K215A
absence of PG		
$K_d = K'_1 K'_2/(1 + K'_2)$ (μM)	7.7 ± 0.6	13 ± 2
$k_+ = k'_2/K'_1$ ($\mu M^{-1} s^{-1}$)	6.1 ± 0.3	3.8 ± 0.2
$k_- = k'_{-2}$ (s^{-1})	38 ± 10	39 ± 4
$k_-/k_+ = K'_1K'_2$ (μM)	6.2	10.3
presence of PG		
$K_d = K'_1K'_2/(1 + K'_2)$ (μM)	50 ± 3[c]	92 ± 10[e]
$k_+ = k'_2/K'_1$ ($\mu M^{-1} s^{-1}$)	4.6 ± 0.6[d]	4.0 ± 0.9[d]
$k_- = k'_{-2}$ (s^{-1})	313 ± 40[d]	212 ± 50[d]
$k_-/k_+ = K'_1K'_2$ (μM)	68	53

[a] In 30% methanol and at 4 °C. $K_i = k_{-i}/k_{+i}$. The parameters k_+ and k_- were obtained assuming a two-step binding kinetics (see above) and from the dependences of k_{obs} upon the ADP concentration (see Figure 1). [b] From ref *3*. [c] Concentration of PG was 0.25 mM. [d] Concentration of PG was 0.2 mM. [e] Concentration of PG was 10 mM.

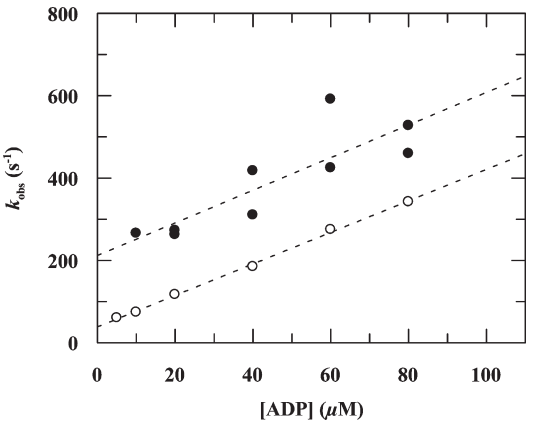

FIGURE 1: Fluorescence stopped-flow experiments with mutant K215A. Dependences of k_{obs} on the ADP concentrations without (○) or with (●) PG. The kinetic parameters obtained (slopes, $k_+ = k'_2/K'_1$; intercepts on the k_{obs} axis, $k_- = k'_{-2}$, Scheme 2) are in Table 1.

Scheme 2: Two-Step Binding Pathway for ADP to PGK

$$E(\cdot PG) \underset{K'_1}{\overset{ADP}{\rightleftharpoons}} E(\cdot PG)\cdot ADP \underset{k'_{-2}}{\overset{k'_2}{\rightleftharpoons}} E^*(\cdot PG)\cdot ADP$$

Because of its low turnover (see below), we attempted to measure the kinetics the formation of the catalytic E**·bPG·ADP with mutant K215A. On mixing E*·bPG with ADP, there was a decrease in fluorescence, but it was difficult to obtain rate constants from the time courses. Nevertheless, the decrease appeared to be as rapid as that observed with the formation of the abortive E*·PG·ADP (data not shown).

From these stopped-flow experiments, it seems that the kinetics of the steps preceding the phospho-transfer step with mutant K215A are as rapid as those with wt PGK. We now investigated the following steps by chemical sampling.

Table 2: Steady-State and Transient Kinetic Parameters for wt PGK and Its Mutant K215A at 4 °C[a]

	forward reaction		backward reaction	
parameter	wt PGK	K215A	wt PGK	K215A
steady-state kinetics				
k_{cat} (s^{-1})	200 ± 10	0.06 ± 0.01	2.48 ± 0.10	0.05 ± 0.01
k_{cat} (s^{-1})[b]	2633 (13)	0.78 (13)	833 (340)	0.48 (10)
K_m (μM)	77 ± 10	126 ± 20	17 ± 1	1600 ± 100
k_{cat}/K_m (μM^{-1} s^{-1})	2.6	4.8×10^{-4}	0.15	3×10^{-5}
transient kinetics[c]				
k_+ (μM^{-1} s^{-1})	2.1 ± 0.3			
k_- (s^{-1})	29 ± 10			
k_-/k_+ (μM)	13.8			
k^{max} (s^{-1})	≫165	0.06 ± 0.01		
$S_{0.5}$ (μM)	≫60	120 ± 30		

[a] In 30% methanol and at 4 °C. [b] In methanol-free buffer and at 20 °C (*16*). Numbers in parentheses are ratios between values obtained in the two different conditions. [c] From single turnovers (Figures 3 and 4; for definitions of constants, see Figure 4 and the text).

(B) Kinetics of Phospho-Transfer and Release of Products Steps: Chemical Sampling. Two types of experiments were carried out. In multiple turnovers, the concentrations of the substrates bPG and ADP were higher than that of PGK. This type enabled us to test for the presence of transient burst phases of ATP formation at different ADP concentrations and to obtain steady-state parameters. In single turnovers, the concentrations of PGK and bPG were the same, but that of ADP was higher and variable. These experiments were carried out by the quench-flow method with PGK + bPG in one syringe and ADP in the other. Flachner et al. (*16*) showed that bPG binds as tightly to mutant K215A as it does to wt PGK (K_d about 50 nM for both), and therefore we assume that under our experimental conditions the concentrations of free enzyme in the multiple turnovers, and of both free enzyme and bPG in the single turnovers, were insignificant.

(C) Multiple Turnover Experiments. The steady-state parameters for wt PGK and mutant K215A have been reported previously in the absence of methanol and at 20 °C: $k_{cat}{}^F = 2633$ and 0.78 s^{-1} and K_m for ADP = 0.12 and 0.15 mM, respectively (*16*). The parameters obtained under our experimental conditions are summarized in Table 2; it is noteworthy that the $k_{cat}{}^F$ for both wt PGK and its mutant are decreased 13-fold by our experimental conditions. We explain this decrease by a similar effect of solvent and temperature (*19*, *20*) on product release with wt PGK and phospho-transfer with the mutant (see following paragraph). On the other hand, the K_m values for ADP are little changed by the experimental conditions.

To allow for the detection of a transient phase of ATP production, one must work at a concentration of PGK that is of the same order of magnitude as ADP. Furthermore, the concentration of ADP must be such that the rate of formation of putative ATP-containing intermediates is higher than the $k_{cat}{}^F$ of wt PGK, that is, 200 s^{-1}. A typical time course for ATP production at a reagent concentration of wt PGK is illustrated in Figure 2a. It shows that the steady state is preceded by a burst of ATP, suggesting that step 3 (phospho-transfer, Scheme 1) is relatively fast and that the steady-state rate is limited by a product release step. We note that the kinetics of the two phases are in reasonable agreement with independent measurements: at 30 μM ADP, $k_{ATP} = 92 \pm 19$ s^{-1} (from the Single Turnover Experiments below) and the steady-state rate = 55 ± 5 s^{-1} (from the steady-state parameters, Table 2).

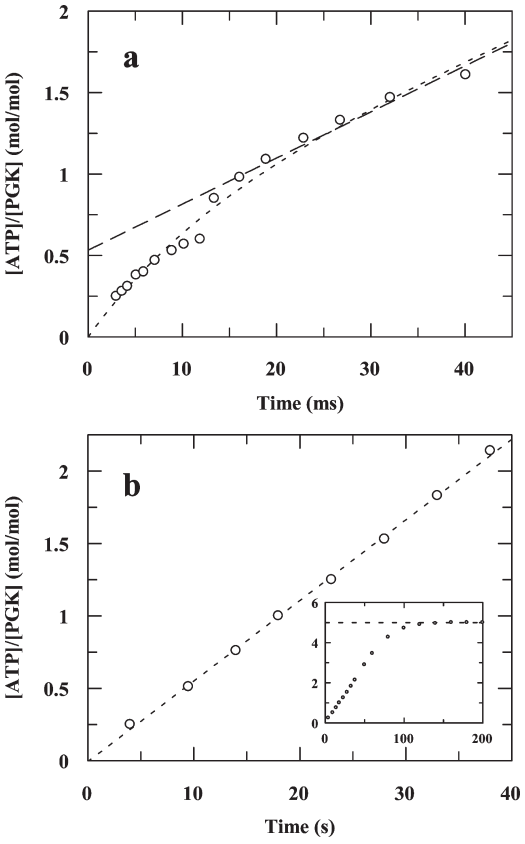

FIGURE 2: Multiple turnover quench-flow experiments with wt PGK (a) and mutant K215A (b) in the forward direction. The reaction mixtures (10 μM PGK, 50 μM bPG, and 30 μM (a) or 1 mM (b) ADP) were quenched in acid at the times indicated, and the ATP was determined. In (a) the time course consists of a transient burst phase of kinetics 80 ± 8 s^{-1} followed by a steady-state phase of rate 28 ± 2 s^{-1}. In (b) the time course consists of a steady-state phase only of rate 0.056 ± 0.005 s^{-1} with the final plateau when all of the bPG had been utilized (inset).

Since the $k_{cat}{}^F$ with mutant K215A is very low (0.06 s^{-1}), it was possible to test for transient phases and to measure the steady-state kinetics on the tens of seconds time scale in the same experiment. A typical time course with the mutant is illustrated in Figure 2b. There are two noteworthy features of this experiment. First, there was no sign of a transient phase. Second, the end point is 50 μM ATP, which corresponds to the initial concentration of bPG (inset in Figure 2b). Further experiments were carried out with ADP in the range 20 μM to 2.5 mM, all at 10 μM mutant K215A and 50 μM bPG: none of the time courses had a transient phase of ATP production, and in each the end point of the time course corresponded to the initial concentration of bPG. Estimates for $k_{cat}{}^F$ and K_m for ADP with the mutant were obtained from the dependence of the initial slope of the time courses on the ADP concentration (Table 2).

From these multiple turnover experiments, we conclude that on the reaction pathway of mutant K215A the steps preceding the phospho-transfer step (steps 1 and 2, Scheme 1) are rapid (absence of transient lag phases) and that intermediates containing ATP do not accumulate (absence of transient burst phases). This is evidence that the phospho-transfer step (step 3, Scheme 1) is rate-limiting, which we tested by single turnover experiments. Thus, we suggest that under single turnover conditions, time courses of ATP formation with the mutant should represent free ATP (kinetics equal to k_{cat}) and with wt PGK, enzyme-bound ATP (kinetics faster than k_{cat}).

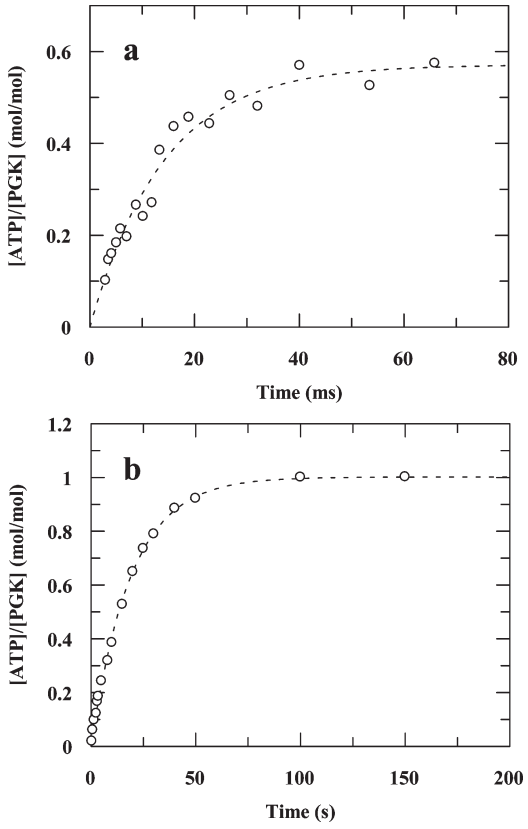

FIGURE 3: Single turnover quench-flow experiments in the forward direction with wt PGK (a) and its mutant (b). The reaction mixtures contained 10 μM PGK, 10 μM bPG, and (a) 30 μM or (b) 1 mM ADP. Each time course was fitted to a single exponential of rate constant k_{ATP}.

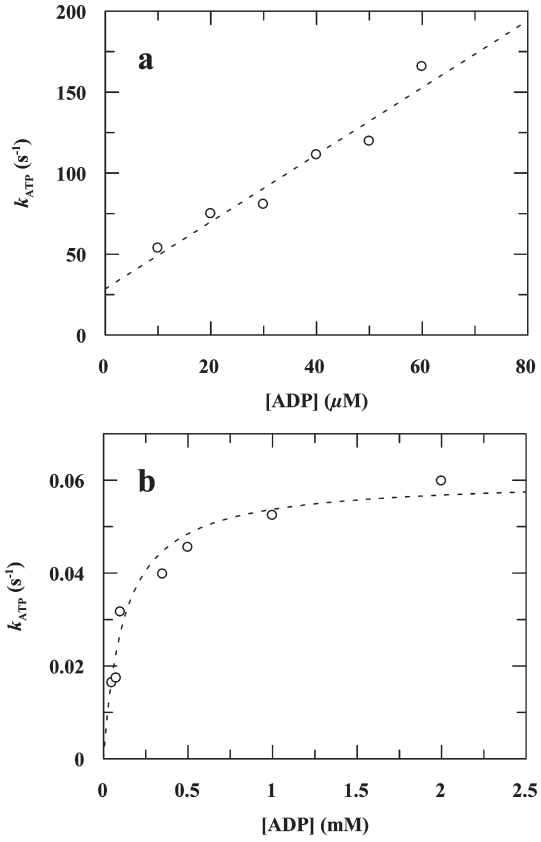

FIGURE 4: ADP dependences of the kinetics in single turnover experiments (k_{ATP}) with wt PGK (a) or mutant K215A (b). In (a), the dependence was fitted to a straight line of slope $k_+ = k_2/K_1$ and intercept on the k_{ATP} axis $k_- = k_{-2}K_3/(1 + K_3)$ (Scheme 1; see Supporting Information for details). In (b), the dependence was fitted to an hyperbola of maximum value $k_{ATP}^{max} = k_3/(1 + K_2)$ and $S_{0.5} = K_1K_2/(1+K_1)$ (Scheme 3; see Supporting Information for details). The constants obtained are in Table 2.

(D) Single Turnover Experiments. Typical single turnover time courses for the formation of ATP by wt PGK and mutant K215A are illustrated in Figure 3. Each time course fitted well to a single exponential of kinetics k_{ATP} and amplitude A_{ATP}. It is noteworthy that transient lag phases were not detected in any of the time courses, whether with wt PGK or its mutant. This confirms that on the time scale of the experiments the steps preceding phospho-transfer (that is, substrate binding, step 1, and the associated conformational changes, step 2, Scheme 2) are rapid equilibria, as already suggested from the fluorescence stopped-flow experiments.

The dependences of k_{ATP} on the ADP concentration were obtained from further ATP burst experiments and are illustrated in Figure 4. With wt PGK (Figure 4a) the dependence is linear and can be described by $k_{ATP} = k_+[ADP] + k_-$, where k_+ is the slope and k_- the intercept on the k_{ATP} axis (values in Table 2). Because the value of the slope, $k_+ = 2.1\ \mu M^{-1}\ s^{-1}$, is too low to represent a diffusion-controlled process (e.g., ref *31*), we assume that ADP binds to E*·bPG in two steps and that $k_+ = k_2/K_1$ (Scheme 1). k_- is a function of k_{-2}, modulated by the equilibrium constants of the following steps.

The maximum value of k_{ATP} measured was 165 s^{-1}; this is somewhat lower than k_{cat}^F (200 s^{-1}), but it was difficult to work at higher ADP concentrations because of the limited time resolution of the quench-flow method. Nevertheless, because of the apparent linearity of the dependence, k_{ATP}^{max} is almost certainly greater than k_{cat}^F. This means that the formation of products during the first catalytic cycle occurs faster than the steady-state rate. Thus, the steady-state rate is limited by another process, presumably product release.

Scheme 3: Forward Reaction Pathway for the K215A Mutant

$$\text{E*·bPG} \underset{K_1}{\overset{\text{ADP}}{\rightleftharpoons}} \text{E*·bPG·ADP} \underset{K_2}{\rightleftharpoons} \text{E**·bPG·ADP} \xrightarrow{k_3} \text{E + PG + ATP}$$

With the mutant, the dependence fitted well to a hyperbola with $k_{ATP}^{max} = 0.06\ s^{-1}$ (Figure 4b). We note that the intercept on the k_{ATP} axis is negligible and that k_{ATP}^{max} is identical to k_{cat}^F. These results support our proposition that the phospho-transfer step is the rate-limiting step on the reaction pathway of mutant K215A. The proposition is further supported by the steps preceding the phospho-transfer (steps 1 and 2, Scheme 1) being rapid equilibria on the time scale of the experiments. Below, by a study of the backward reaction, we give evidence that the following steps are rapid equilibria, too. Accordingly with the mutant, we can reduce Scheme 1 to Scheme 3.

In this scheme the predominant intermediate in the steady-state is E**·bPG·ADP; the concentrations of the enzyme product complexes are low because they dissociate much more rapidly than they are formed. With mutant K215A, therefore, free ATP is produced in a virtually irreversible process which is confirmed by the negligible intercept in the k_{ATP} axis in ADP dependence of k_{ATP} (Figure 4b) and the high amplitudes in the single turnovers (Figure 3b).

By Scheme 3, $k_{cat}^F = k_{ATP}^{max} = k_3/(1 + K_2) = 0.06\ s^{-1}$ and $K_m^{ADP} = S_{0.5} = K_1K_2/(1 + K_2) = 120\ \mu M$ (Table 2; see Supporting Information for details).

Kinetic Studies on the Backward Reaction (bPG Formation). It was not possible to study the substrate binding steps in the backward reaction (steps 4 and 5, Scheme 1) because although there was a fluorescence signal upon mixing PGK (whether the wild-type or mutant) with ATP, the amplitude of the signal was low and the kinetics difficult to obtain with our stopped-flow equipment. Therefore, our work on the backward reaction was restricted to chemical sampling experiments.

We summarize in Table 2 the steady-state parameters for both wild-type PGK and its mutant in the backward reaction: as in the forward reaction, k_{cat} with the mutant is very low. Under the experimental conditions of Flachner et al. (*16*), $k_{cat}^{B} = 833\ s^{-1}$ with wt PGK and $0.48\ s^{-1}$ with mutant K215A. The K_m values for ATP were 0.11 and 2.47 mM, respectively, in reasonable agreement with our estimates (Table 2). However, under our experimental conditions, the k_{cat}^{B} of wt PGK was 340-fold lower than that under the condition of Flachner et al., whereas in the forward reaction the reduction was only 13-fold. The k_{cat}^{B} found by Flachner et al. is relatively high because, unlike under our conditions, it was obtained under anion activating conditions that accelerate the otherwise slow bPG release kinetics (*21*). On the other hand, with mutant K215A k_{cat}^{B} at 4 °C is only 10-fold less than at 20 °C because the phospho-transfer step, which is not subjected to anion activation, is rate-limiting (see below).

Typical time courses for ADP production with wt PGK and its mutant at high enzyme concentrations under multiple turnover conditions are illustrated in Figure 5. With wt PGK (Figure 5a), the time course consisted of a transient burst phase of ADP that is followed by a short steady-state phase leading to the final equilibrium (final plateau not shown).

With the mutant (Figure 5b), each of the two time courses consisted of an initial linear phase that was followed by a gradual decrease to a plateau as the final equilibrium was attained. There are two noteworthy features of these experiments. First, the linear phases agreed well with the steady-state rates expected from the steady-state measurements (Table 2): at 0.5 mM ATP, $0.010\ s^{-1}$, expected $0.012\ s^{-1}$; at 1 mM ATP, $0.015\ s^{-1}$, expected $0.019\ s^{-1}$. Second, neither time course displayed a transient phase. This is evidence that on the time scale of the experiments the initial ATP binding kinetics are fast (otherwise there would have been a transient lag) and that ADP-containing complexes do not accumulate in the steady state (which would have resulted in a burst phase).

The result of these multiple turnover experiments is evidence that the phospho-transfer step in the backward reaction is rate-limiting, as it is in the forward reaction. Unfortunately, in the backward reaction we were unable to confirm the slowness of the phospho-transfer by single turnovers because of the poor binding of ATP [$K_d = 2.5$ mM (*16*)]. Thus, these experiments require high concentrations of ATP, high enough to compete with PG (unpublished results) whose concentration is equal to that of the mutant and therefore low.

Because the ADP release kinetics appear to be fast (as evidenced from the results of the stopped-flow experiments), we propose Scheme 4 as a reaction pathway for mutant K215A in the backward reaction.

By the same arguments as for the forward reaction, $k_{cat}^{B} = k_{-3}/(1 + K_4) = 0.05\ s^{-1}$ and $K_m^{ATP} = K_4K_5/(1 + K_4) = 1.6$ mM.

Probing the Residual Phosphotransferase Activities of Mutant K215A. Flachner et al. (*16*) showed that mutant K215A is not completely inactive in that it possesses a low phosphotransferase activity in both the forward and backward reactions. We confirm here this finding under our experimental conditions.

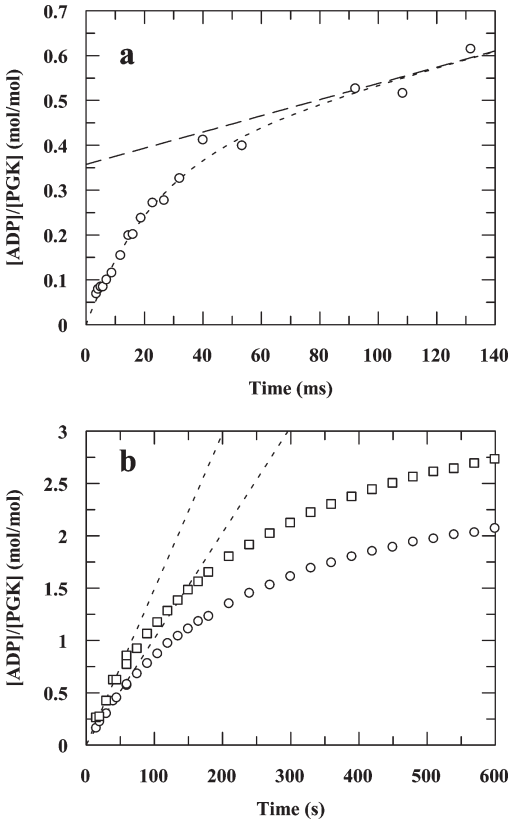

FIGURE 5: Multiple turnover quench-flow experiments in the backward reaction with wt PGK (a) or mutant K215A (b). The reaction mixtures contained 10 μM PGK, 5 mM PG, and (a) 60 μM or (b) 0.5 mM (○) and 1 mM ATP (□). In (a) the time course was fitted to a single exponential followed by a linear phase, the slope of which (shown as dashed line) corresponds to the steady-state rate. In (b) the initial time courses were fitted to straight lines.

Scheme 4: Backward Reaction Pathway for the K215A Mutant

$$\mathrm{E^{*}{\cdot}PG} \overset{\mathrm{ATP}}{\underset{K_5}{\rightleftharpoons}} \mathrm{E^{*}{\cdot}PG{\cdot}ATP} \rightleftharpoons \mathrm{E^{**}{\cdot}PG{\cdot}ATP} \xrightarrow[K_4]{k_{-3}} \mathrm{E + bPG + ADP}$$

A cause of concern with mutants of very low turnovers is that the activities measured are due to a contaminating enzyme. In enzymes that involve ADP, adenylate kinase, which has a high turnover, can be troublesome. Here, we exclude this contamination because the end points in the steady-state time courses correspond to the initial concentration of bPG and not that of ADP (except at concentrations of ADP less than that of bPG). Further, when ADP was incubated with mutant K215A in the absence of bPG on the time scale of our experiments, there was no production of ATP (data not illustrated). Another potential contaminant is PGK from the *Escherichia coli* used in the preparation of the mutant. In this event, the single turnover experiments would have been carried out under multiple turnover conditions (that is, with the concentration of any contaminating PGK less than those of the bPG and ADP) which would have resulted in linear time courses. As the time courses were exponentials, we can exclude that the activity measured comes from a contaminating *E. coli* PGK. We conclude that mutant K215A possesses a low intrinsic phosphotransferase activity. Below, we try to understand the mechanism of this reaction with *in silico* experiments.

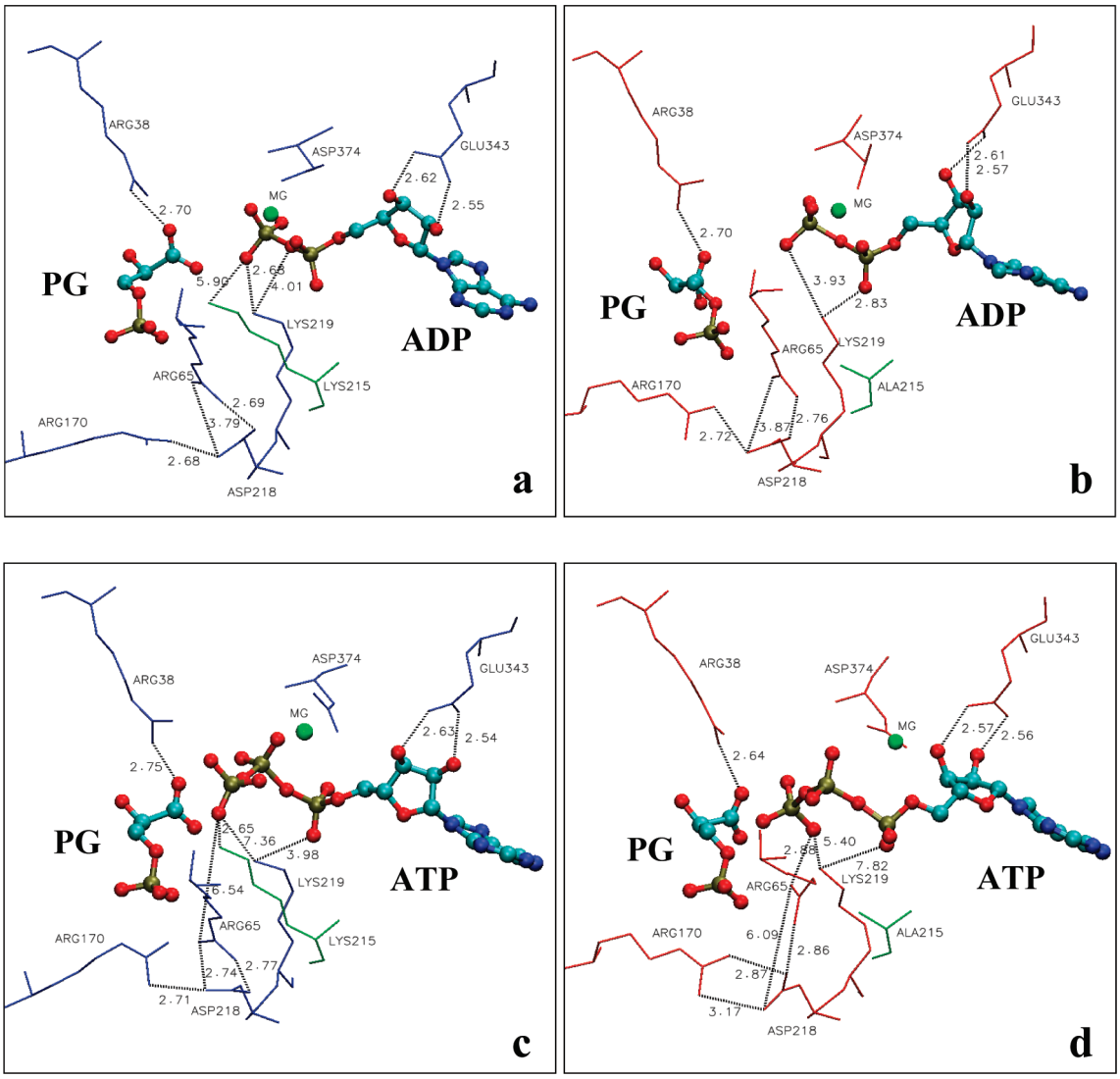

FIGURE 6: Docking of ADP and ATP to wt PGK and mutant K215A. For each docking the closed conformation of PGK was used, and PG was already bound to the enzyme. Nucleotide binding site for ADP onto (a) wt PGK and (b) mutant K215A and for ATP onto (c) wt PGK and (d) mutant K215A. The distances between ligands and the protein residues are given in Table 3. The ligands are in ball and stick model; Lys 215, Ala 215, and Mg^{2+} are shown in green.

Table 3: Distances (Å) between Substrates (PG, ADP, or ATP) and Protein Residues in the Two Modeled Ternary Complexes of wt PGK or Mutant K215A[a]

nucleotide groups		γ-phosphate (oxygen)	2′-OH (ribose)	3′-OH (ribose)	γ-phosphate (oxygen)	α-phosphate (oxygen)	γ-phosphate (oxygen)		
PG	oxygen of C1								
PGK residues	Arg 38 (α 1A)	Arg 65 (β B)	Glu 343 (β J)	Glu 343 (β J)	Lys 215 (α 8)	Lys 219 (α 8)	Lys 219 (α 8)	Asp 218 Arg 65	Asp 218 Arg 170
with PG and ADP									
wt	2.70		2.55	2.62		4.01		2.69/3.79	2.68/5.24
K215A	2.70		2.57	2.61		2.83		2.76/3.87	2.72/5.01
with PG and ATP									
wt	2.75	**6.54**	2.54	2.63	2.65	3.98	**7.36**	2.74/2.77	2.71/4.92
K215A	2.64	**2.88**	2.56	2.57		7.82	**5.40**	2.86/6.09	2.87/3.17

[a] Numbers in bold are discussed in the text. α and β denote α-helix and β-strand (or loop after the β-strand), respectively.

Molecular Modeling, Docking of ADP and ATP in the Closed Conformation of PGK, and Dynamics. The closed structure of hPGK, whether wild-type or mutant K215A, was modeled using the *T. brucei* PGK structure (13PK). ADP or ATP and PG were docked on these modeled structures. The binding modes of ADP to wt PGK and its mutant K215A in the presence of PG (to form the abortive complex E*·PG·ADP which is thought to be in the closed conformation of PGK) are very similar, as shown by the interactions observed between substrates and protein residues (Figure 6a,b and Table 3). A key feature of the closed conformation of PGK is present, namely, the salt bridge between Asp 218 and Arg 65 (*14*). As expected, the binding

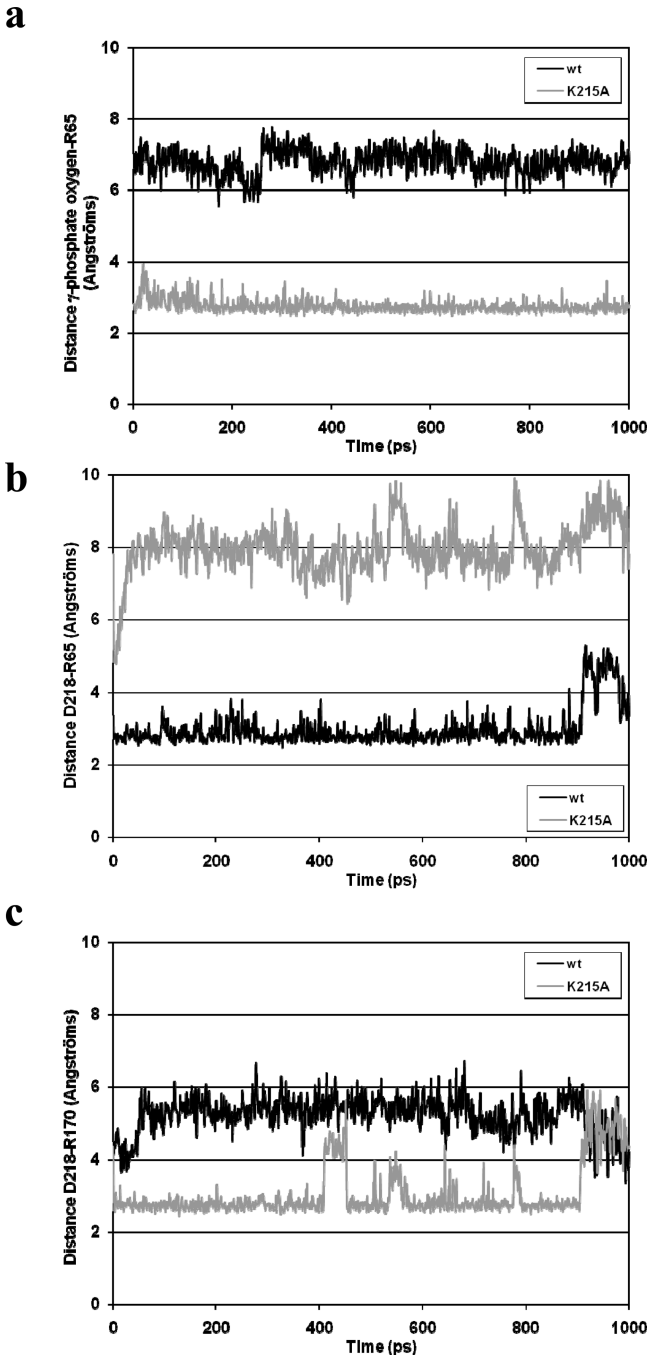

FIGURE 7: Molecular dynamics. (a) Distances measured between the γ-phosphate oxygen and the Arg 65 side chain during the molecular dynamics simulation for the closed conformation of wt PGK (black trace) and mutant K215A (gray trace). Distances of the salt bridges observed between Asp 218 and either (b) Arg 65 or (c) Arg 170 during the simulation.

mode of ADP is indifferent to the presence of Lys 215. The binding of the ribose moiety to Glu 343 is very similar for the two proteins (Table 3). In contrast, the binding of ATP (Figure 6c,d) shows significant differences. First, in the mutant, Lys 219 is closer to the γ-phosphate oxygen of ATP than with the wt PGK (7.36 and 5.40 Å for wt and mutant, respectively, Table 3). Second, with wt PGK, Lys 215 interacts strongly with the γ-phosphate oxygen, whereas interestingly with the mutant, Arg 65 takes the place of Lys 215 for this interaction. Arg 65 belongs to the "basic patch" that is part of the PG site (*5*). With the mutant, Arg 65 interacts with both Asp 218 and the γ-phosphate oxygen of ATP. The distances between Arg 65 and the γ-phosphate oxygen were 6.54 and 2.88 Å for wt and mutant, respectively. Therefore, in both structures, the closed conformation appears to be preserved (salt bridge between Arg 65 and Asp 218) and the γ-phosphate stabilized (interaction with either Lys 215 for the wt PGK or Arg 65 for the mutant K215A). The presence of this latter interaction in the mutant might explain the residual activity of the K215A enzyme.

In order to make sure that these interactions are not temporary connections that could be unstable over time, a short molecular dynamics run was carried out. First, the interaction between the γ-phosphate oxygen and Arg 65 was found to be stable for mutant K215A with an average distance of 2.75 Å (Figure 7a). As expected, for wt PGK this distance was large (around 7 Å). Surprisingly, with the mutant, Asp 218 which was primarily interacting with Arg 65 was found to interact with Arg 170 (Figure 7b,c). Whereas the distance between Asp 218 and Arg 65 was originally 2.88 Å (before the dynamics, Table 3), this value increased up to 8 Å at the beginning of the simulation and remained constant during 1 ns. Finally, the connection between Asp 218 and Arg 170, which is fluctuating for wt PGK, was found to be more stable over time for the mutant. This new salt bridge probably helps to stabilize the closed conformation of the mutant.

IMPLICATIONS AND CONCLUSIONS

It has been proposed that the active site of kinases includes a positively charged amino acid residue that plays a crucial role in the phospho-transfer process by stabilizing the putative transition state (*32*−*34*). O'Brien et al. (*33*) suggest that the guanidinium group of arginine is especially suitable for the binding a phospho group, and they give a list of kinases that have an arginine residue at their active sites. Here with PGK, we cannot exclude that Arg 38 plays a role in the phospho-transfer process, as it has been proposed to be catalytically important (*17*). On the other hand, certain protein kinases possess a lysine residue at their active sites. Thus, Taylor et al. (*35*) showed that cAMP-dependent protein kinase has two lysine residues that are catalytically important: Lys 72 that binds the α- and β-phosphates of ATP and, in particular, Lys 168 that binds the γ-phosphate and may be involved in the phospho-transfer step itself. Carrera et al. (*36*) proposed that the phospho-transfer step of protein kinase (tyrosine) involves a lysine residue. Here we show by a kinetic study that Lys 215 plays a crucial role in the phospho-transfer step of hPGK. Nevertheless, mutant K215A, although highly inefficient, is still able to transfer the 1-phospho group of bPG to the β-phosphate of ADP, and we must address the origin of this low activity.

From our control experiments, the activity of the mutant does not appear to be due to a contaminating enzyme. Therefore, we must consider the possibility that in the mutant Lys 215 is to a limited extent replaced by another basic amino acid residue that interacts with the 1-phospho group of bPG (or the γ-phosphate of ATP in the backward reaction). Szabó et al. (*17*) suggest that the nearby Lys 219 may be implicated in the phospho-transfer process of PGK. Here we support this suggestion by molecular modeling, namely, that in the mutant Lys 219 is close to the γ-phosphate of ATP. However, according to the distance estimated between Lys 219 and ATP (~4 Å), this interaction alone may not be strong enough to support phospho-transfer.

Another candidate to explain the phospho-transfer activity of mutant K215A is Arg 65. Several works show that this arginine is not essential for the catalytic activity of yPGK (*37*−*39*). However, in the absence of Lys 215, it could be that Arg 65 is involved

in the phospho-transfer process or, at least, that it stabilizes the phosphate chain in a proper position which would allow this step to occur. Thus, from our docking and molecular dynamics study we show that, in the closed structure of mutant K215A, Arg 65 is near the γ-phosphate of ATP, a position that may explain the residual phospho-transfer activity of the mutant. It has to be underlined that the closed structures are modeled by homology to another PGK species and therefore should be considered with care. Furthermore, our theoretical study shows that in the mutant the salt bridge between Arg 65 and Asp 218 is disrupted and replaced by a bridge between Asp 218 and Arg 170 that appears to be stable during the 1 ns simulation. Interestingly, in the *T. brucei* PGK closed structure, the corresponding arginine, Arg 172, is also located very near to Asp 218 (4.89 Å).

Whichever residue substitutes for Lys 215, or even if a basic amino acid residue is not necessary at all, we suggest that the phospho-transfer is the rate-limiting step on the overall reaction pathway of mutant K215A. Thus with the mutant in the steady-state, the predominant intermediate in the forward reaction is E**·bPG·ADP and in the backward reaction, E**·PG·ATP. With wild-type PGK, it is the product's release kinetics that are rate-limiting in both reactions.

ACKNOWLEDGMENT

We are grateful to the Centre de Biochimie Structurale (UMR5048, CNRS, INSERM U554) in Montpellier for the use of the circular dichroism apparatus. We thank Dr. Lionel Verdoucq (UMR5004, INRA, Montpellier) for the use of the cell disruptor and technical advice.

SUPPORTING INFORMATION AVAILABLE

Circular dichroism spectra of wt PGK and mutant K215A in the two different buffers used in this study (without methanol or with 30% methanol), dependences of the amplitude of the substrate-induced fluorescence change of mutant K215A on the ADP concentration in the absence or presence of PG, and equations and derivatives used for determining the different constants of substrate binding kinetics and single turnover experiments. This material is available free of charge via the Internet at http://pubs.acs.org.

REFERENCES

1. Scopes, R. K. (1973) 3-Phosphoglycerate kinase. *Enzymes (3rd Ed.) 8*, 335–351.
2. Schlichting, I., and Reinstein, J. (1997) Structures of active conformations of UMP kinase from *Dictyostelium discoideum* suggest phosphoryl transfer is associative. *Biochemistry 36*, 9290–9296.
3. Gondeau, C., Chaloin, L., Varga, A., Roy, B., Lallemand, P., Perigaud, C., Barman, T., Vas, M., and Lionne, C. (2008) Differences in the transient kinetics of the binding of D-ADP and its mirror image L-ADP to human 3-phosphoglycerate kinase revealed by the presence of 3-phosphoglycerate. *Biochemistry 47*, 3462–3473.
4. Lay, A. J., Jiang, X. M., Kisker, O., Flynn, E., Underwood, A., Condron, R., and Hogg, P. J. (2000) Phosphoglycerate kinase acts in tumour angiogenesis as a disulphide reductase. *Nature 408*, 869–873.
5. Harlos, K., Vas, M., and Blake, C. F. (1992) Crystal structure of the binary complex of pig muscle phosphoglycerate kinase and its substrate 3-phospho-D-glycerate. *Proteins 12*, 133–144.
6. Davies, G. J., Gamblin, S. J., Littlechild, J. A., Dauter, Z., Wilson, K. S., and Watson, H. C. (1994) Structure of the ADP complex of the 3-phosphoglycerate kinase from *Bacillus stearothermophilus* at 1.65 Å. *Acta Crystallogr., Sect. D: Biol. Crystallogr. 50*, 202–209.
7. Flachner, B., Kovári, Z., Varga, A., Gugolya, Z., Vonderviszt, F., Náray-Szabó, G., and Vas, M. (2004) Role of phosphate chain mobility of MgATP in completing the 3-phosphoglycerate kinase catalytic site: binding, kinetic, and crystallographic studies with ATP and MgATP. *Biochemistry 43*, 3436–3449.
8. Varga, A., Flachner, B., Konarev, P., Gráczer, É., Szabó, J., Svergun, D., Závodszky, P., and Vas, M. (2006) Substrate-induced double sided H-bond network as a means of domain closure in 3-phosphoglycerate kinase. *FEBS Lett. 580*, 2698–2706.
9. Gondeau, C., Chaloin, L., Lallemand, P., Roy, B., Périgaud, C., Barman, T., Varga, A., Vas, M., Lionne, C., and Arold, S. T. (2008) Molecular basis for the lack of enantioselectivity of human 3-phosphoglycerate kinase. *Nucleic Acids Res. 36*, 3620–3629.
10. Kovári, Z., Flachner, B., Náray-Szabó, G., and Vas, M. (2002) Crystallographic and thiol-reactivity studies on the complex of pig muscle phosphoglycerate kinase with ATP analogues: correlation between nucleotide binding mode and helix flexibility. *Biochemistry 41*, 8796–8806.
11. May, A., Vas, M., Harlos, K., and Blake, C. (1996) 2.0 Å resolution structure of a ternary complex of pig muscle phosphoglycerate kinase containing 3-phospho-D-glycerate and the nucleotide Mn adenylylimidodiphosphate. *Proteins 24*, 292–303.
12. Szilágyi, A. N., Ghosh, M., Garman, E., and Vas, M. (2001) A 1.8 Å resolution structure of pig muscle 3-phosphoglycerate kinase with bound MgADP and 3-phosphoglycerate in open conformation: new insight into the role of the nucleotide in domain closure. *J. Mol. Biol. 306*, 499–511.
13. Bernstein, B. E., Michels, P. A., and Hol, W. G. (1997) Synergistic effects of substrate-induced conformational changes in phosphoglycerate kinase activation. *Nature 385*, 275–278.
14. Auerbach, G., Huber, R., Grattinger, M., Zaiss, K., Schurig, H., Jaenicke, R., and Jacob, U. (1997) Closed structure of phosphoglycerate kinase from *Thermotoga maritima* reveals the catalytic mechanism and determinants of thermal stability. *Structure 5*, 1475–1483.
15. White, E. M., Holland, A. R., and MacDonald, G. (2008) Infrared studies reveal unique vibrations associated with the PGK-ATP-3-PG ternary complex. *Biochemistry 47*, 84–91.
16. Flachner, B., Varga, A., Szabó, J., Barna, L., Hajdú, I., Gyimesi, G., Závodszky, P., and Vas, M. (2005) Substrate-assisted movement of the catalytic Lys 215 during domain closure: Site-directed mutagenesis studies of human 3-phosphoglycerate kinase. *Biochemistry 44*, 16853–16865.
17. Szabó, J., Varga, A., Flachner, B., Konarev, P. V., Svergun, D. I., Závodszky, P., and Vas, M. (2008) Communication between the nucleotide site and the main molecular hinge of 3-phosphoglycerate kinase. *Biochemistry 47*, 6735–6744.
18. Douzou, P. (1977) Enzymology at subzero temperatures. *Adv. Enzymol. Relat. Areas Mol. Biol. 45*, 157–272.
19. Geerlof, A., Schmidt, P. P., Travers, F., and Barman, T. (1997) Cryoenzymic studies on yeast 3-phosphoglycerate kinase. Attempt to obtain the kinetics of the hinge-bending motion. *Biochemistry 36*, 5538–5545.
20. Geerlof, A., Travers, F., Barman, T., and Lionne, C. (2005) Perturbation of yeast 3-phosphoglycerate kinase reaction mixtures with ADP: transient kinetics of formation of ATP from bound 1,3-bisphosphoglycerate. *Biochemistry 44*, 14948–14955.
21. Scopes, R. K. (1978) Binding of substrates and other anions to yeast phosphoglycerate kinase. *Eur. J. Biochem. 91*, 119–129.
22. Tucker, J., Sczakiel, G., Feuerstein, J., John, J., Goody, R. S., and Wittinghofer, A. (1986) Expression of p21 proteins in *Escherichia coli* and stereochemistry of the nucleotide-binding site. *EMBO J. 5*, 1351–1358.
23. Vas, M., and Batke, J. (1984) Adenine nucleotides affect the binding of 3-phosphoglycerate to pig muscle 3-phosphoglycerate kinase. *Eur. J. Biochem. 139*, 115–123.
24. Sali, A., and Blundell, T. L. (1993) Comparative protein modelling by satisfaction of spatial restraints. *J. Mol. Biol. 234*, 779–815.
25. Humphrey, W., Dalke, A., and Schulten, K. (1996) VMD: visual molecular dynamics. *J. Mol. Graphics 14*, 33–38, 27−38.
26. Phillips, J. C., Braun, R., Wang, W., Gumbart, J., Tajkhorshid, E., Villa, E., Chipot, C., Skeel, R. D., Kale, L., and Schulten, K. (2005) Scalable molecular dynamics with NAMD. *J. Comput. Chem. 26*, 1781–1802.
27. Brooks, B. R., Brooks, C. L. III, Mackerell, A. D. Jr., Nilsson, L., Petrella, R. J., Roux, B., Won, Y., Archontis, G., Bartels, C., Boresch, S., Caflisch, A., Caves, L., Cui, Q., Dinner, A. R., Feig, M., Fischer, S., Gao, J., Hodoscek, M., Im, W., Kuczera, K., Lazaridis, T., Ma, J., Ovchinnikov, V., Paci, E., Pastor, R. W., Post, C. B., Pu, J. Z., Schaefer, M., Tidor, B., Venable, R. M., Woodcock, H. L., Wu, X., Yang, W., York, D. M., and Karplus, M. (2009) CHARMM: the biomolecular simulation program. *J. Comput. Chem. 30*, 1545–1614.
28. Merli, A., Szilágyi, A. N., Flachner, B., Rossi, G. L., and Vas, M. (2002) Nucleotide binding to pig muscle 3-phosphoglycerate kinase in

the crystal and in solution: relationship between substrate antagonism and interdomain communication. *Biochemistry 41*, 111–119.
29. Barman, T. E., Bellamy, S. R., Gutfreund, H., Halford, S. E., and Lionne, C. (2006) The identification of chemical intermediates in enzyme catalysis by the rapid quench-flow technique. *Cell. Mol. Life Sci. 63*, 2571–2583.
30. Wiksell, E., and Larsson-Raznikiewicz, M. (1982) Substrate binding to phosphoglycerate kinase monitored by 1-anilino-8-naphthalenesulfonate. *J. Biol. Chem. 257*, 12672–12677.
31. Gutfreund, H. (1995) Kinetics for the Life Sciences, Cambridge University Press, Cambridge.
32. Matte, A., Tari, L. W., and Delbaere, L. T. (1998) How do kinases transfer phosphoryl groups? *Structure 6*, 413–419.
33. O'Brien, P. J., Lassila, J. K., Fenn, T. D., Zalatan, J. G., and Herschlag, D. (2008) Arginine coordination in enzymatic phosphoryl transfer: evaluation of the effect of Arg166 mutations in *Escherichia coli* alkaline phosphatase. *Biochemistry 47*, 7663–7672.
34. Vetter, I. R., and Wittinghofer, A. (1999) Nucleoside triphosphate-binding proteins: different scaffolds to achieve phosphoryl transfer. *Q. Rev. Biophys. 32*, 1–56.
35. Taylor, S. S., Radzio-Andzelm, E., and Hunter, T. (1995) How do protein kinases discriminate between serine/threonine and tyrosine? Structural insights from the insulin receptor protein-tyrosine kinase. *FASEB J. 9*, 1255–1266.
36. Carrera, A. C., Alexandrov, K., and Roberts, T. M. (1993) The conserved lysine of the catalytic domain of protein kinases is actively involved in the phosphotransfer reaction and not required for anchoring ATP. *Proc. Natl. Acad. Sci. U.S.A. 90*, 442–446.
37. Barber, M. D., Gamblin, S. J., Watson, H. C., and Littlechild, J. A. (1993) Site-directed mutagenesis of yeast phosphoglycerate kinase. Arginines 65, 121 and 168. *FEBS Lett. 320*, 193–197.
38. McPhillips, T. M., Hsu, B. T., Sherman, M. A., Mas, M. T., and Rees, D. C. (1996) Structure of the R65Q mutant of yeast 3-phosphoglycerate kinase complexed with Mg-AMP-PNP and 3-phospho-D-glycerate. *Biochemistry 35*, 4118–4127.
39. Sherman, M. A., Dean, S. A., Mathiowetz, A. M., and Mas, M. T. (1991) Site-directed mutations of arginine 65 at the periphery of the active site cleft of yeast 3-phosphoglycerate kinase enhance the catalytic activity and eliminate anion-dependent activation. *Protein Eng. 4*, 935–940.